Supporting information

Sol-gel Synthesis Control of Iron-Cobalt Alloy/Ferrite Core/shell Nanoparticles Supported by a Carbon Medium with Semi-Hard Magnetic Features

Alberto Castellano-Soria[1,2,*], Jesús López-Sánchez[3,4], Aida Serrano[5], Giulio Gorni[6,7], María Varela[2,8], Ignacio Sardinero[4], Noemí Carmona[1,2], Antonio Hernando[1,2], Pilar Marín,[1,2] and Elena Navarro[1,2]

[1] Instituto de Magnetismo Aplicado (IMA-UCM-ADIF), 28230 Madrid, Spain

[2] Departamento de Física de Materiales, Facultad de Físicas, Universidad Complutense de Madrid (UCM), 28040 Madrid, Spain

[3] SpLine, Spanish CRG BM25 Beamline, ESRF-The European Synchrotron, 38000 Grenoble, France

[4] Instituto de Ciencia de Materiales de Madrid (ICMM-CSIC), 28049 Madrid, Spain

[5] Instituto de Cerámica y Vidrio (CSIC), 28049 Madrid, Spain

[6] CELLS-ALBA Synchrotron Light Facility, E-08290 Cerdanyola del Vallès, Spain

[7] Instituto de Óptica (IO-CSIC), 28006, Madrid, Spain

[8] Instituto Pluridisciplinar, Universidad Complutense de Madrid (UCM), 28040 Madrid, Spain

*Corresponding author: albcas04@ucm.es

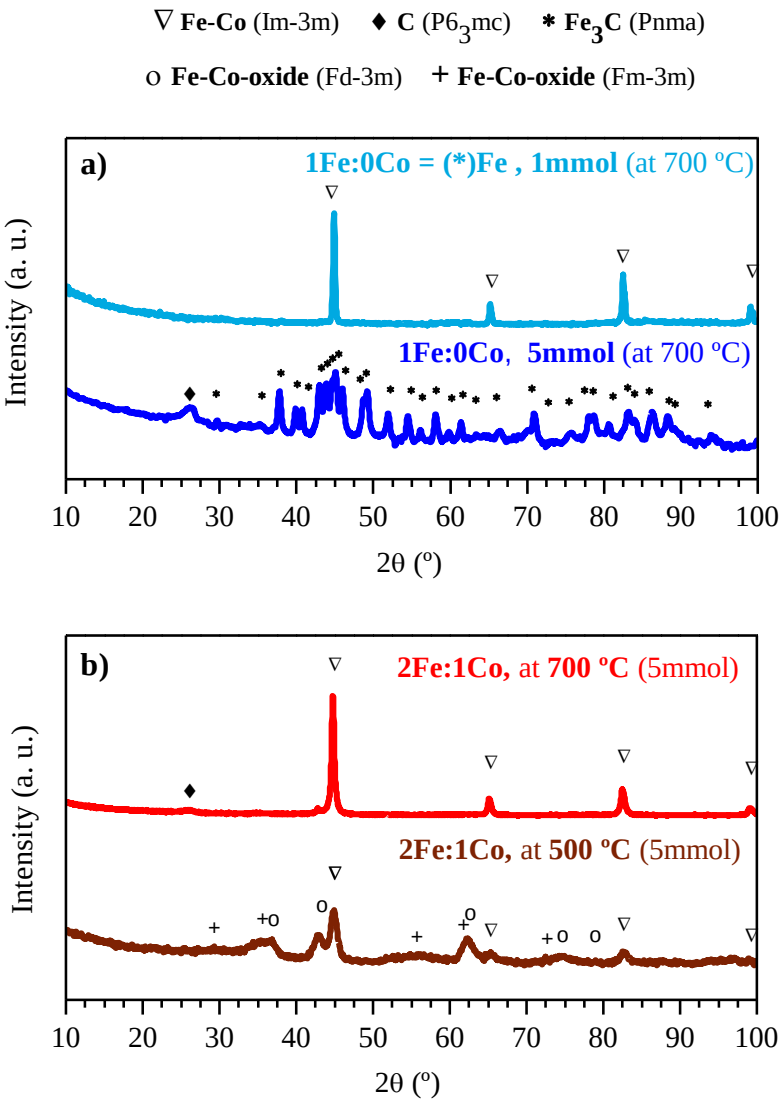

Figure 1. Conventional X-ray diffractograms (Cu $K_{\alpha1}/K_{\alpha2} = 2$, $\lambda = 1.542$ Å) of two different samples. a) 1Fe:0Co samples densified at the same temperature (700 ºC) from xerogels prepared with 1 mmol (renamed as (*)Fe sample) and 5 mmol of organic surfactants. b) XRD evolution with the densification temperature, from oxides (500 ºC) to a high metallic phase (700 ºC), for the 2Fe:1Co sample.

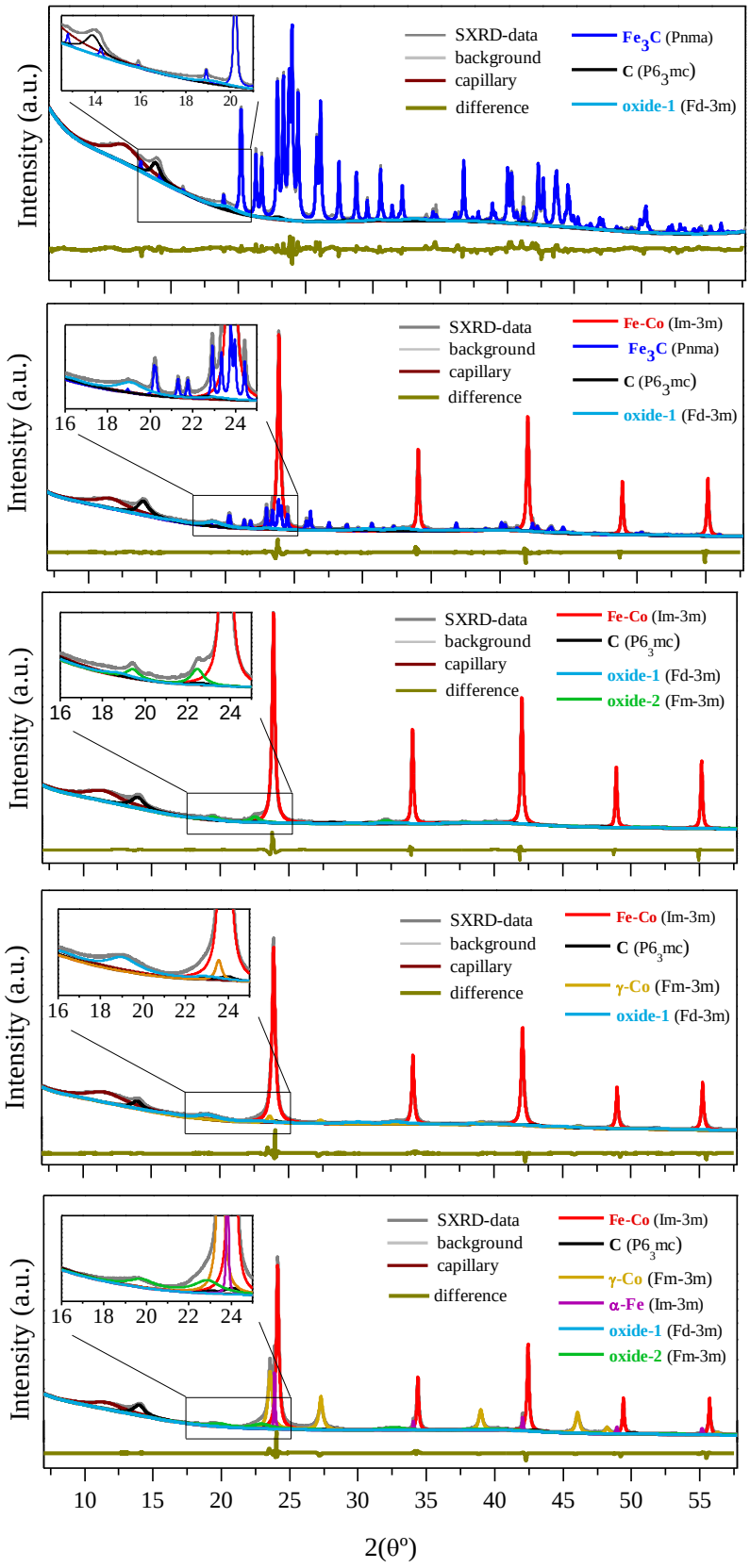

Figure 2. Rietveld refinements for the synchrotron X-ray diffractograms of the samples: 1Fe:0Co, 19Fe:1Co, 5Fe:1Co, 2Fe:1Co and 1Fe:2Co, respectively. The experimental data, background and the capillary-amorphous contributions are printed in dark-grey, grey, and red-wine colors. The contribution of the adjusted phases to the total diffractogram are shown in different colors at the right column of the legend. The difference between the Rietveld model and the experimental data is shown in gray-yellow color at the bottom of each graph.

C-P63mc				Fe3C				FeCo				Co				Fe				oxide-1				oxide-2			
l. v. (Å)		**% wt.**	**size (nm)**	**l. v. (Å)**		**% wt.**	**size (nm)**	**l. v. (Å)**		**% wt.**	**size (nm)**	**l. v. (Å)**		**% wt.**	**size (nm)**	**l. v. (Å)**		**% wt.**	**size (nm)**	**l. v. (Å)**		**% wt.**	**size (nm)**	**l. v. (Å)**		**% wt.**	**size (nm)**
1Fe:0Co																											
a	2.553(5)	24(2)	5.1(2)	a	5.093(1)	72(2)	28.1(1)	-				-				-				-	4(1)	3(1)		-			
c	6.924(4)			b	6.749(1)																						
				c	4.529(1)																						
19Fe:1Co																											
a	2.558(4)	26(2)	4.6(2)	a	5.087(1)	11(1)	28.2(4)	a	2.86876(2)	53(1)	27.7(5)	-				-				-	8(1)	1.8(5)		-			
c	6.890(3)			b	6.751(1)																						
				c	4.528(1)																						
5Fe:1Co																											
a	2,595(8)	27(2)	3.7(1)	-				a	2.86829(2)	68(2)	29.0(1)	-				-				-	2(1)	1.8(6)	a	4.297(3)	4.5(2)	4(1)
c	6.895(4)																										
2Fe:1Co																											
a	2,570(9)	25(1)	5.7(3)	-				a	2.86448(3)	63(1)%	21.7(1)	a	3.55(9)	2.3(1)	8(3)	-				a	8.404(1)	8(1)	2.3(8)	-			
c	6.897(6)																										
1Fe:2Co																											
a	2.590(9)	37(1)	4.6(2)	-				a	2.84135(4)	37(1)%	25.7(1)	a	3.559(3)	16.9(2)	11.2(3)	a	2.867(1)	2.1(1)	49(3)	-	2(1)	1.8(5)	a	4.232(3)	4.7(3)	2(1)
c	6.893(5)																										

Figure 3. Results of the Rietveld refinements models for the synchrotron X-ray diffractograms of the samples: 1Fe:0Co, 19Fe:1Co, 5Fe:1Co, 2Fe:1Co and 1Fe:2Co, respectively. Lattice vectors, compositional percentage, and crystalline size of each phase.

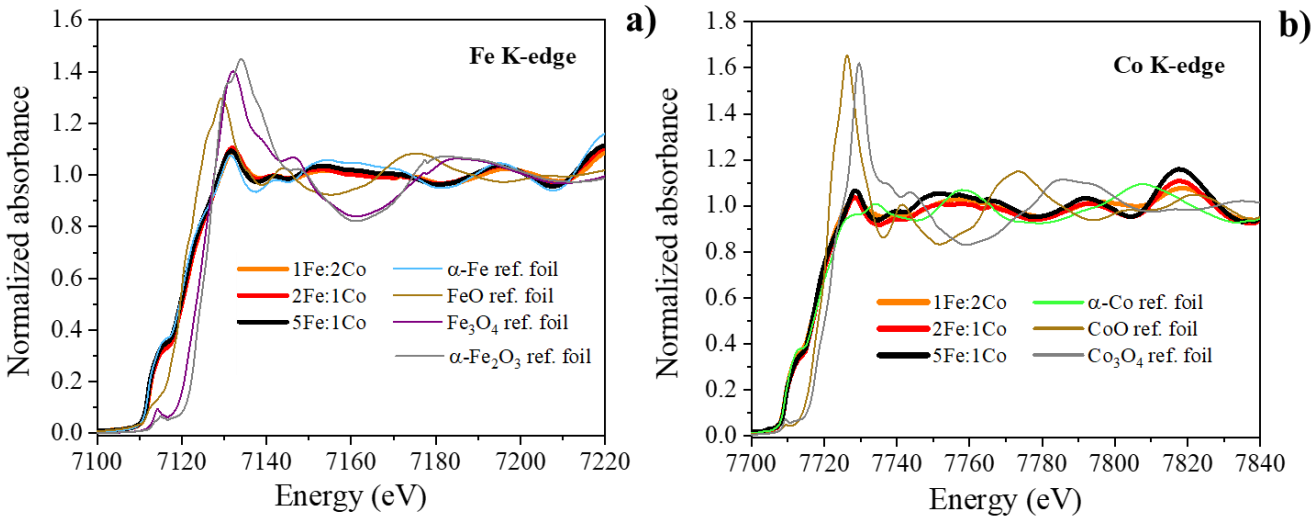

Figure 4. XANES spectra of different references foils along with the three samples studied. a) and b) at the Fe and Co K-edge absorption edge showing their respective set of oxides: {FeO, α-Fe_2O_3, Fe_3O_4} and {CoO, Co_3O_4}.

Law-approach-to-saturation fitting method (LAS). At the high applied field region, the changes in magnetization are small and the main contribution of magnetization arises from rotation mechanisms, and hence, an estimation of the magnetic anisotropy only coming from crystal anisotropy is obtained. As Akulov demonstrated [1], the $M(H)$ at a high field applied can be approximated by: $M(H) \propto M_s\left(1-\frac{a}{H}-\frac{b(K)}{H^2}\right)$, where a is a parameter related with the leakage field from ferromagnetic materials following the Néel's theory [2] and $b(K) \propto \frac{K^2}{(M_s H)^2}$ for cubic NPs with randomly oriented easy axis [3]. We calibrate the $M(H)$ equation computing the proportional factor *d* by fitting our hysteresis loop data of the *Fe sample, introducing the well-known value reported in the literature of K = 46.8 kJ/m^3 for α-Fe at 300 K [4]:

$$M(H) = M_s\left(1-\frac{a}{H}-d\left(\frac{K}{M_s H}\right)^2\right) \quad (1)$$

Fixing the obtained value of $d = 57$ are determined the values of K for Fe:Co samples.

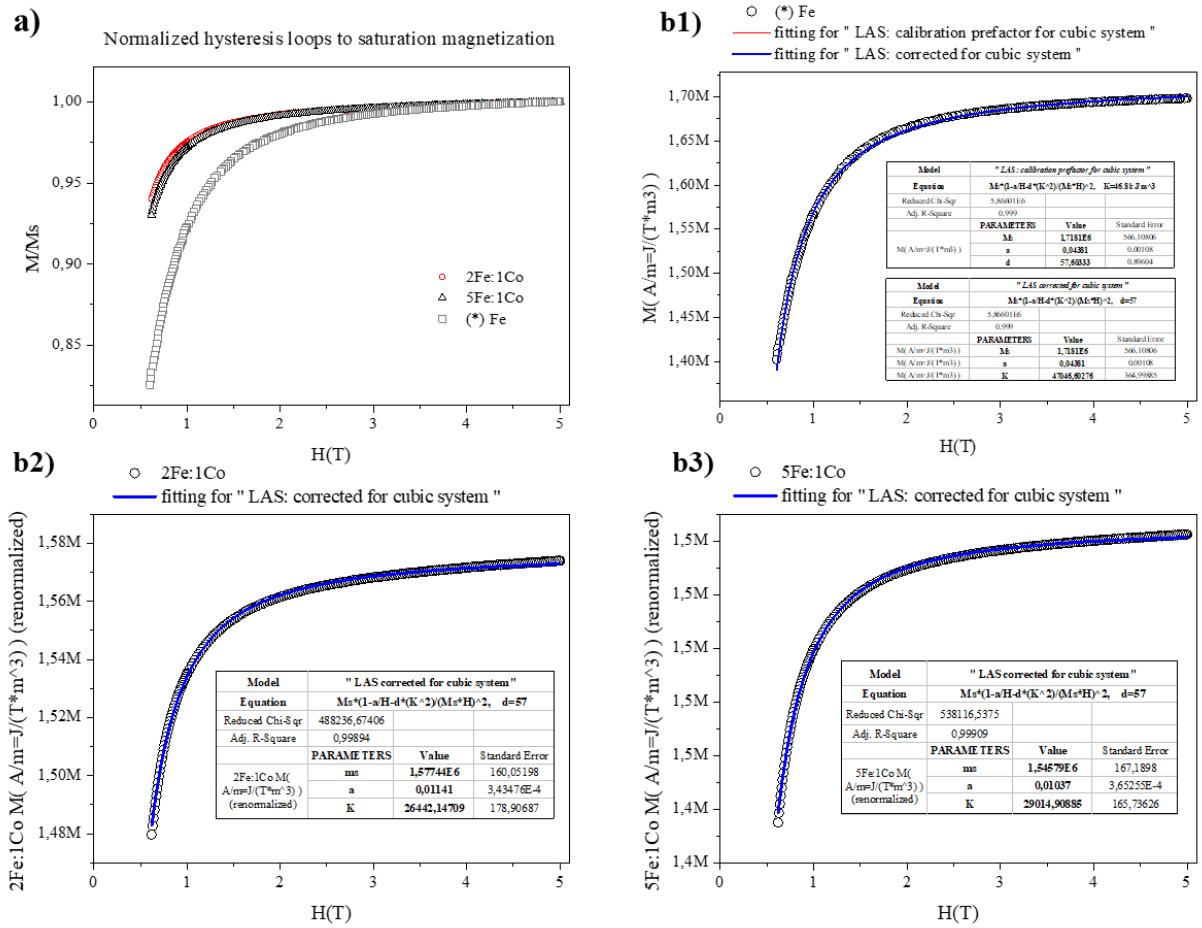

Model	" LAS corrected for cubic system "		
Equation	Ms*(1-a/H-d*(K^2)/(Ms*H)^2, d=57		
Reduced Chi-Sqr	488236,67406		
Adj. R-Square	0,99894		
	PARAMETERS	Value	Standard Error
2Fe:1Co M(A/m=J/(T*m^3)) (renormalized)	ms	1,57744E6	160,05198
	a	0,01141	3,43476E-4
	K	26442,14709	178,90687

Model	" LAS corrected for cubic system "		
Equation	Ms*(1-a/H-d*(K^2)/(Ms*H)^2, d=57		
Reduced Chi-Sqr	538116,5375		
Adj. R-Square	0,99909		
	PARAMETERS	Value	Standard Error
5Fe:1Co M(A/m=J/(T*m^3)) (renormalized)	ms	1,54579E6	167,1898
	a	0,01037	3,65255E-4
	K	29014,90885	165,73626

Figure 5. Law-approach-to-saturation fitting method at the high applied field region for the first quadrant branch of hysteresis loops taken at 300 K. a) Normalized curves for the (*)Fe, 2Fe:1Co, and 1Fe:2Co samples showing a softer magnetic character for such (*)Fe sample. (b) Fitting for the *d* parameter with the (*)Fe sample by a known anisotropy constant value of K=46.8 kJ/m^3. (b2), (b3) Fittings of K values for the curves of the samples 2Fe:1Co and 1Fe:2Co, respectively

References.

[1] N.S. Akulov, Über den Verlauf der Magnetisierungskurve in starken Feldern, Zeitschrift Für Physik 1931 69:11. 69 (1931) 822–831. https://doi.org/10.1007/BF01339465.

[2] L. Néel, Relation entre la constante d'anisotropie et la loi d'approche à la saturation des ferromagnétiques, Journal de Physique et Le Radium. 9 (1948) 193–199. https://doi.org/10.1051/JPHYSRAD:0194800906019300.

[3] J. Herbst, F. Pinkerton, Law of approach to saturation for polycrystalline ferromagnets: Remanent initial state, Phys Rev B. 57 (1998) 10733. https://doi.org/10.1103/PhysRevB.57.10733.

[4] B. Westerstrand, P. Nordblad, L. Nordborg, The Magnetocrystalline Anisotropy Constants of Iron and Iron-silicon Alloys, Phys Scr. 11 (1975) 383. https://doi.org/10.1088/0031-8949/11/6/010.